p722 ferrocifen loaded lipid nanocapsules improve survival of murine xenografted-melanoma via a potentiation of apoptosis and an activation of CD8+ T lymphocytes

Solène Topin-Ruiz, Adélie Mellinger, Elise Lepeltier, Clara Bourreau, Juliette Fouillet, Jeremie Riou, Gérard Jaouen, Ludovic Martin, Catherine Passirani, Nicolas Clere

p722 ferrocifen loaded lipid nanocapsules improve survival of murine xenografted-melanoma *via* a potentiation of apoptosis and an activation of $CD8^+$ T lymphocytes

Solène Topin-Ruiz[1,2*], Adélie Mellinger[1*], Elise Lepeltier[1], Clara Bourreau[1], Juliette Fouillet[1], Jérémie Riou[1], Gérard Jaouen[3,4], Ludovic Martin[2], Catherine Passirani[1], Nicolas Clere[1]

(1) MINT, Univ Angers, INSERM, CNRS, IBS-CHU, 4 rue Larrey, F-49933 Angers, France

(2) Centre Hospitalier Universitaire, service de dermatologie, 4 rue Larrey, F-49933 Angers, France

(3) PSL, Chimie ParisTech, Paris Cedex 05, France

(4) Sorbonne Université, CNRS, Institut Parisien de Chimie Moléculaire (IPCM, UMR 8232), Paris Cedex 05, France

(*) These authors contributed equally

Conflicts of interest: None

Corresponding author
Nicolas CLERE – Pharm D., Ph D
UMR Inserm 1066 – CNRS 6021
IBS – IRIS
CHU
4, rue Larrey
F-49933 ANGERS Cedex
nicolas.clere@univ-angers.fr

Word numbers: Abstract (177 words); Text (5,912 words);

References (41);

Number of Figures (6); Number of table (1)

Table of abbreviations

AUC : Area under the curve

Bax : Bcl2-associated protein X

BCl-2 : B-cell lymphoma 2

CTLA-4 : Cytotoxic T-lymphocyte associated protein 4

DMSO : Dimethyl-sulfoxide

DSPE-PEG : 1, 2-Distearoyl-sn-glycero-3-phosphoethanolamine-Poly(ethylene glycol)

HBSS : Hank's Balanced Salt Solution

LNC : Lipid nanocapsules

mAb : Monoclonal antibody

MeOH : Methanol

MEK : Mitogen-activated extracellular signal-regulated protein kinase

NaCl : Sodium chloride

PBS : Phosphate buffered saline

PD-1 : Programmed cell death protein 1

PEG : Polyethylene glycol

PdI : Polydispersity index

ROS : Reactive oxygen species

RPMI : Roswell Park Memorial Institute medium

UPLC : Ultra Performance Liquid Chromatography

Highlights

- p722-LNC induces a significant decrease of B16F10 melanoma cell viability
- p722-LNC slows tumor growth and improves the survival of treated mice
- Antitumor activities of p722-LNC are explained by a potentiation of intrinsic apoptotic pathway and an activation of $CD8^+$ T lymphocytes

Abstract

Metastatic melanoma is a malignant tumor with a poor prognosis. Recent new therapeutics improved the survival of patients at a metastatic stage. However, the low response rate to immunotherapy, explained in part by resistance to apoptosis, needs to develop new strategies. The ferrocifen family represents promising bioorganometallic molecules for melanoma treatment since they show potent anticancer properties. The aim of this study is (i) to evaluate the benefits of a strategy involving encapsulated p722 in lipid nanocapsules (LNC) in B16F10 melanoma mice models and (ii) to compare the beneficial effects with an existing therapy such as anti-CTLA4 mAb. Interestingly, LNC-p722 induces a significant decrease of melanoma cell viability. *In vivo* data shows a significant improvement in the survival rate and a slower tumor growth with p722-loaded LNC in comparison with anti-CTLA4 mAb. Western blots confirm that LNC-p722 potentiates intrinsic apoptotic pathway. Treatment with LNC-p722 significantly activates $CD8^+$ T lymphocytes compared to treatment with anti-CTLA4 mAb. This study uncovers a new therapeutic strategy with encapsulated p722 to prevent B16F10 melanoma growth and to improve survival of treated mice.

Keywords: Ferrocifen, metastatic melanoma, CD8 T lymphocytes, apoptosis

Introduction

Cutaneous cancers are among the most common cancers, with more than two to three million new cases around the world each year. The incidence of melanoma increased dramatically over the past 50 years [1]. Although it accounts for 5% of all skin cancers, cutaneous melanoma is responsible for 75% of skin cancer deaths. The survival rate of melanoma varies depending on the stage of the disease at the time of prognosis. Thus, overall relative survival rate at any stage is 97% at one year, 85% at five years while, in metastatic conditions, the median survival is six to nine months.

Where melanoma is concerned, the difficulties of early dissemination and pronounced chemotherapy resistance remained completely unsolved for decades [2]. Since 2011, the situation has improved due to the development of new targeted therapies such as BRAF or MEK inhibitors and efficient immune-stimulating antibodies such as anti-CTLA4, anti-PD1 or anti-PDL1. Several mechanisms have been linked to CTLA4-mediated activities [3]. During native T cell activation, the expression of CTLA4 protein on the cell surface is upregulated and directly competes with the CD28 protein in binding with the CD80 and CD86 molecules [4]. The inhibitory signals from CTLA4 can also prevent the activation of self-reactive T cells by attenuating T cell signaling. These strategies lead to a significant increase in metastatic melanoma patients‘overall survival time [5;6]. Nevertheless, for many patients, tumor relapses and therapy resistance often follow within only a few months or years, after an initial tumor reduction phase [7;8]. Thus, new therapeutic strategies are still needed, which may further improve the clinical outcome. Many drug candidates have been investigated and metal-based drugs, particularly ferrocifen-based drugs, represent a promising family of anticancer compounds [9;10].

The bioorganometallic molecules are active molecules containing at least one carbon atom directly bound to a metal or metalloid. In ferrocifens, the metal studied is iron and the metallocene derivative is ferrocene chemically grafted onto a polyphenolic skeleton, resulting in ferrocenyl phenol derivatives [11]. In recent years, our group has demonstrated, through tumor-xenografted mice model, the beneficial effects of ferrociphenol on the tumor cell apoptosis or senescence in triple negative breast cancer [12] or in melanoma [10]. Furthermore, cytotoxic properties of ferrocifens have been reported through an increase in the production of reactive oxygen species (ROS) [13] and the generation of an active redox metabolite that interact selectively with nucleophilic biomolecules such as glutathione or the thioredoxin reductase. However, due to their hydrophobicity, the use of lipid core vectors such as lipid nanocapsules (LNC), allows an optimal encapsulation and an intravenous administration of these molecules [14].

Among the therapeutic strategies for melanoma, immunotherapy has a key role for several years. Thus, a significant improvement of the median overall survival has been observed after treatment with ipilimumab, a monoclonal antibody against cytotoxic T-lymphocyte antigen-4 (CTLA-4), which is able to exploit the natural ability of the immune system to eradicate primary cancer cells [7]. Furthermore, it has been reported the benefit of the combination of anti-CTLA4 antibodies and radiotherapy in metastatic melanoma. Thus, a median survival prolongation of 3 to 5 months and response rates of 25.7 *vs* 6.5% have been observed in anti-CTLA4 groups [15]. Taken together, these studies confirm the interest of using anti-CTLA4 antibodies to treat metastatic melanoma.

The aim of this study was to evaluate the benefits of a strategy involving encapsulated p722 in LNC in B16F10 melanoma mice models. For the first time, an increase in therapeutic efficacy was observed in LNC-p722 treated mice in comparison with anti-CTLA mAb treated

mice. Interestingly, LNC p722 is able to improve survival of murine xenografted-melanoma *via* a potentiation of apoptosis and an activation of $CD8^+$ T lymphocytes

Materials and methods

Chemical materials

p722 (Fig. 1) was synthesized according to the protocol from Pigeon *et al*. [16]. The lipophilic Labrafac® WL1349 (caprylic-capric acid triglycerides) was purchased from Gatefossé S.A. (Saint-Priest, France). Lipoid® S75-3 (soybean lecithin at 69% of phosphatidylcholine came from Lipoid GmbH (Ludwigshafen, Germany), Kolliphor®HS15 is a mixture of polyglycol mono- and di-esters of 12-hydroxystearic acid and of about 30% of free polyethylene glycol (BASF, Ludwigshafen, Germany), and NaCl from Prolabo (Fontenay-sous-bois, France). Deionised water was acquired from Milli-Q system (Millipore, Paris, France). DSPE-mPEG2000 (Mean Molecular Weight, MMw = 2805 $g.mol^{-1}$) was provided by Avanti Polar Lipids (Alabaster, USA).

Formulation of p722-loaded lipid nanocapsules (p722-LNC)

The LNC vehicle was formulated in accordance with a phase inversion method, as previously described[17]. Firstly, all the excipients were mixed (16.9% w/w Kolliphor®HS15 (BASF, Ludwigshafen, Germany), 1.5% w/w Lipoid®S75-3 (Lipoid GmbH, Ludwigshafen, Germany), 20.6% w/w Labrafac® (caprylic-capric acid triglycerides, Gatefossé S.A. Saint-Priest, France), 1.8% w/w NaCl (Prolabo, Fontenay-sous-Bois, France) and 59.2% w/w water (obtained from a Milli-Q system, Millipore, Paris, France)) under magnetic stirring and heated from room temperature to 60°C for 15 min. Three temperature cycles between 60 and 90 °C were performed to obtain phase inversions of the emulsion. Secondly, when the temperature was

in the phase inversion zone (73-78°C), ice-cold water was added (88.4%v/v) to induce irreversible shock and dilution, and to form the LNC suspension. The nanocapsules were stored at 4°C. To formulate p722-LNC, 0.5% w/w p722 powder (concentration at 2.35 mM) was added at step I, with all the excipients and the formulation process was the same as for empty LNC. To separate free p722 from p722-loaded lipid nanocapsules, the suspension was passed through 0.2 µm cellulose acetate filter.

Post-insertion of DSPE-PEG

The polymer used for post-insertion was 1,2-distearoyl-sn-glycero-3-phosphoethanolamine-N- [methoxy(polyethyleneglycol)-2000] (DSPE-mPEG2000) (Avanti Polar Lipids, Inc, Alabaster, USA). DSPE-mPEG2000 and LNC were co-incubated for 4h at 37 °C, with a final polymer concentration adjusted to 5 mM. At this concentration, the post-insertion is total [18] and the number of DSPE-mPEG2000 molecules per LNC is around 3 [19].

Characterization of p722-LNC: size and zeta potential

The mean diameter and polydispersity index (PdI) of LNC were characterized by using Dynamic Light Scattering (DLS) from a Malvern Zetasizer® apparatus (Nano Series ZS, Malvern Instruments S.A., Worcestershire, UK) at 25 °C, after dilution by 100 with UPW. The measured average values were calculated from 3 runs, with 10 measurements per run.

The zeta potential of the nanocapsules was determined by laser Doppler micro-electrophoresis using a Zetasizer Nano ZS system (Nano Series ZS, Malvern Instruments S.A., Worcestershire, UK) [20].

Characterization of p722-LNC: encapsulation efficiency (EE)

The encapsulated p722 concentration was directly measured by quantifying p722 in the LNC using a supplier recommended UPLC method (Waters, France). For this purpose, the LNCs were broken via a dilution by 10 in methanol (VWR international, Fontenay-sous-bois, France). A BEH C18 analytical column (2.1 x 50 mm, 1.7 µm, Waters, France) was used at room temperature. DMSO (Thermofisher, Kandel, Germany) and MeOH were used as mobile phases (isocratic mode: 10:90, 10 min). The flow rate was 0.2 $mL.min^{-1}$, injection volume was 2 µL and p722 was quantified by a UV detector at a wavelength of 450 nm. Analysis of the data was performed by Empower 3 software (Waters). Calibration curves were established by quantifying the area under the curves (AUCs) of 0-200 $\mu g.mL^{-1}$ solutions of p722 in DMSO and MeOH 10:90.

Encapsulation efficiency, EE (%), was calculated using the following equation:

$$EE\ (\%) = \frac{(Encapsulated\ p722\ conc.\ in\ LNC)\ \times\ 100}{Initial\ p722\ conc.\ in\ LNC}$$

Drug loading, DL (% w/w), was calculated using the following equation:

$$Drug\ loading\ (\%\ w/w) = \frac{(Mass\ of\ encapsulated\ p722\ in\ 1\ mL\ of\ LNC\ dispersion)\ \times 100}{Total\ mass\ of\ excipients\ and\ p722\ in\ 1\ mL\ of\ LNC\ dispersion}$$

Cell culture

B16F10 mouse melanoma cell lines (gift from University of Brussels) were grown in RPMI-1640 medium (Lonza, Verviers, Belgium) supplemented with 10% fetal bovine serum (Biowest, Nuaillé, France), 1% non-essential amino acid (Lonza, Walkersvill, USA), 10 units of penicillin and 10 mg of streptomycin (Sigma-Aldrich, Saint Louis, USA). B16F10 was cultured according to ATCC protocol and maintained at 37°C in a humidified atmosphere with 5% CO_2.

Determination of cell viability

B16F10 cells were seeded onto 96-well plates at a density of $5x10^4$ cells/well and precultured overnight. Cells were treated with p722, empty PEG-LNC ("blank") and p722 PEG-LNC for 24 h at a concentration range from 10^{-4} to 100 mg/mL[10]. Cytotoxicity tests were performed using the MTT assay. The OD was evaluated by Multiskan Ascent (Labsystems, Fischer Scientific, Wilmington, USA) at 492 nm.

***In vivo* tumor development**

Ethical approval

All procedures involving animals, including the breeding protocols, were conducted in accordance with protocols approved by the ethical committee of the University of Angers and the regional ethics committee on animal testing (APAFIS#6540-2017012017467029v1). Furthermore, animal experiments were carried out in strict accordance with recommendations in the guidelines of the Code for Methods and Welfare Considerations in Behavioral Research with Animals (Directive 2010/63/UE).

Orthotopic model of B16F10 melanoma

C57BL/6 mice were housed at the university animal facility (Service Commun d'Animalerie Hospitalo-Universitaire; Université d'Angers, France) and were distributed in cages (4 mice/cages). A syngenic, allograft model of melanoma was obtained by subcutaneously injecting a suspension of 10^6 B16F10 melanoma cells in 100 µL of HBSS with calcium and magnesium (Lonza, Walkersvill, Etats-Unis) into the right flank of mice. Before injecting cells, mice were anesthetized with isoflurane (isoflurane was chosen because it induced rapid and reversible anesthesia). Tumor size and tumor volume were monitored until the end of the

protocol and have been estimated using the formula: $V=\pi/6 \times L \times W^2$ (L: length and W: Width). When the tumor volume was approximately 100 mm^3, mice were treated according to the following protocol.

The treatment of mice was randomized and was administrated blind. When tumor volume was around 100 mm^3 (day 0), mice were treated, with intraperitoneal injections of PEG-p722-LNC (7 mg/kg) – to limit the first-pass hepatic effect - or blank PEG-LNC, daily from day 1 to day 5 at the beginning of the afternoon. Otherwise, mice were treated with anti-CTLA4 monoclonal antibody (10 mg/kg) on days 2, 4 and 6. At the end of the protocol, mice were sacrificed (animals were anesthetized with isoflurane and then, euthanized by CO_2), and tumors were removed, frozen and stored at -80°C. In accordance with ethical rules, the animals were sacrificed when the tumor volume was greater than 2500 mm^3 or when the animals showed signs of suffering.

Western blot

For the *in vitro* protocol, proteins were extracted from cells by scrapping with a cell lysis buffer (10 mmol/L Tris-Base, 1 mmol/L Na_3O_4 and 1% SDS, pH 7.4). For the *in vivo* protocol, mice tumors were grinded with Ultra-turrax in the same lysis buffer. Twenty micrograms of proteins were resolved in 10% (*v*/*v*) SDS-PAGE gel and transferred onto a nitrocellulose membrane (0.45 µm pore size) (Amersham GE Healthcare). Mouse anti-Bcl-2 (ab694, Abcam) and rabbit anti-Bax (ab32503, Abcam), anti-Procaspase 9 (ab138412, Abcam), anti-Caspase 9 (ab 202068, Abcam), anti-Procaspase 3 (ab 183179, Abcam) and anti-caspase 3 (ab 184787, Abcam) were used as primary antibodies. A second mouse (goat anti-mouse IgG, secondary antibody, HRP conjugate, Life Technologies) and rabbit (61-6520, Invtrogen) antibodies were used. Detection (using LAS4000, GE HealthCare) was performed using

enhanced chemoluminescence (ECL; Fisher Scientific, Pierce). In each case, protein levels were normalized to the housekeeping protein actin and the protein expression fold differences, between treated and control conditions, were plotted by ImageJ software.

Immunophenotyping of mice lymphocytes

To analyze the composition of mouse lymphocytes, blood samples were collected on days 1 and 9 (from the venous sinus) and at the end of the protocol (from a cardiac puncture). They were diluted into a staining buffer (PBS, pH 7.0 plus 1% fetal calf serum) and cells were stained with fluorescent-label CD3, CD8 and CD69 antibodies (BD Biosciences) for 45 min on ice, followed by two washes in the staining buffer. Then, the cells were subjected to flow cytometry analyses (PACEM platform, SFR ICAT, University of Angers, Angers, France).

Statistical analysis

Results were expressed as a median. For the *in vitro* study, statistical significance between control and treated groups was evaluated using a Mann-Whitney test.

For the *in vivo* study, the statistical tests were performed with the R software. The tumoral growth analysis was performed thanks to a linear mixt model (longitudinal data), including the time influence (intra and inter day variability) and random intercept (intra and inter individual variability). In order to obtain a reliable statistical model, the tumoral volume was converted into a decimal logarithmic scale. Survival analysis was done using a log rang model to compare survival curves and to calculate survival medians.

The significance threshold was defined at p value ≤ 0.05 for each statistical test.

Results

Physico-chemical properties of lipid nanocapsules

The p722 concentration into LNC was settled at 2.35 nM. At this concentration, the encapsulation efficiency was 65% and the drug loading reached 0.7%. Hydrodynamic diameter and zeta potential of the LNC suspensions are summarized in Table 1. The p722 entrapment into LNC did not modify the diameter compared to empty LNC. The size of PEGylated LNC (unloaded or loaded with p722) showed a increase (of around 20 nm), attributed to the surface decoration by the PEG shell [18]. The zeta potential represents the apparent surface charge. The p722 entrapment did not modify the zeta potential compared to blank LNC. LNC PEGylation decreased the zeta potential ~~from -5 mV to~~ (-29 mV and -13 mV) for unloaded and ~~from -6 mV to -13 mV for~~ loaded LNC (Table 1), respectively, due to the electrical dipole of ethylene glycol moiety. The different suspensions have a polydispersity index < 0.2, an important parameter illustrating the monodispersity of the suspension. The stability of loaded LNC was assessed at 4°C (storage condition) for 3 weeks: the hydrodynamic diameter, polydispersity index, zeta potential, entrapment encapsulation and drug loading were not modified (Fig.S1A-C).

Ferrocifen activity on melanoma cell viability and cell apoptosis

Free p722 had a significant cytotoxicity with an IC_{50} estimated at 0.09 mg/mL (corresponding to 1.68 x 10^{-4} M). Encapsulated p722 (p722-LNC) had the same toxicity profile as the free drug (IC_{50} = 0.10 mg/mL corresponding to 1.87 x 10^{-4} M), evidencing the capacity of LNC to deliver ferrocifen into B16F10 melanoma cells without additional toxicity. In addition, for blank LNC, IC_{50} was significantly increased (2.90 mg/mL *i.e.* 54.16 x 10^{-4} M) compared to free or encapsulated p722 (Fig. 2A).

As shown in Fig. 2B, the Western blot analysis revealed that Bax, pro-caspase 9, cleaved caspase 9 and pro-caspase 3 were found at higher levels in B16F10 cells under free p722 exposure compared with untreated cells. Furthermore, in these experimental conditions, no difference in cleaved caspase 3 expression has been observed in cells treated with free p722 in comparison to untreated cells. This same experiment was carried out with p722-pegylated LNC. No modification in the expression of Bcl2, Bax and cleaved caspase 3 was demonstrated. However, an increase of pro-caspase 9, cleaved caspase 9 and pro-caspase 3 was found in comparison with untreated cells. ~~Furthermore, no modification of expression of the different proteins was shown in the presence of pegylated LNC without p722 (Fig. 3B).~~

Anti-tumor efficacy of ferrocifens on a mouse model of melanoma

Due to the absence of a significant difference in the volumes of tumors isolated from treated mice, an analysis of the growth rate was considered; the final point chosen was the critical tumor volume of 2,500 mm^3. It was reported that this critical tumor volume was more rapidly observed for mice treated with anti-CTLA4 mAb. Conversely, this critical tumor volume was evolving more slowly in mice treated with p722-pegylated LNC compared to mice treated with blank LNC (Fig. 3A).

Moreover, in mice with melanoma, treatment with p722-pegylated LNC significantly improved their survival compared to mice treated with blank LNC (22 days *versus* 13 days of survival, respectively) (Fig. 3B). No difference was observed for mice treated with anti-CTLA mAb in comparison with blank LNC (Fig. 3C) while a significant difference was found in the survival of mice treated with p722-pegylated LNC in comparison with anti-CTLA4 mAb (Fig. 3D).

Ferrocifen loaded LNC potentiate apoptosis via the intrinsic pathway

As shown in Fig. 4, no difference was found in the expression of the different proteins tested both in tumors from mice treated with anti-CTLA4 mAb or anti-CTLA4 mAb and p722-pegylated LNC compared to control mice. However, a significant increase in pro-caspase 9, cleaved caspase 9, pro-caspase 3 and cleaved caspase 3 has been observed in tumors from mice treated with p722-pegylated LNC in comparison with control mice.

Ferrocifen loaded LNC potentiate the activation of CD_8^+ T lymphocytes

Quantification of CD_8^+ T lymphocytes was conducted on mice blood samples at different times (day 0, day 9 and at the end of the *in vivo* protocol). As described in Fig. 5A, no difference in the percentage of CD_8^+ T lymphocytes was observed whatever the time and treatments. No difference was found at day 0 and at the end of the protocol in the percentage of activated CD_8^+ T lymphocytes. However, a significant increase of activated CD_8^+ T lymphocytes has been shown, at day 9, in blood samples from mice treated with p722-pegylated LNC or p722-pegylated LNC and anti-CTLA4 mAb (Fig. 5B).

Discussion

Because numerous preclinical and clinical studies focused on the analysis of innovative combinatory therapeutic [21];[22] in melanoma therapy, the main objective of the present work is to evaluate the therapeutic properties of p722, a new promising molecule from the ferrocifen family, encapsulated in LNC, in a mouse metastatic melanoma model. Furthermore, the secondary objective is to compare the therapeutic benefits of p722-LNC with a recognized therapeutic strategy using anti-CTLA4 antibody. Interestingly, a significant improvement in the survival rate and a slower tumor growth were found with p722 loaded LNC compared to anti-CLTA4 treatment. These data were supplemented by Western blot analyzes which confirmed that p722-LNC potentiates apoptosis by enhancing the intrinsic pathway. Furthermore, treatment with p722-LNC potentiates the activation of $CD8^+$ T lymphocytes suggesting new properties for these promising encapsulated antitumor molecules.

In the ferrocifen family, the key motif is [ferrocenyl-ene-phenol] leading to the formation of ferrocenyl quinone methides by oxidation on cancer cells. ~~Chemically, this new functional group behaves as a selective electrophile that can react with a variety of nucleophiles [23].~~ At the biological level, the entity offers some new perspectives, inducing very low IC_{50} values, between 0.03 to 0.5 µM, on a range of cancer cells including some resistant to coordination complexes of Pt^{2+} [16]. It operates by apoptosis and/or senescence. Inhibition of pluripotent cancer stem-cells by ferrociphenols has also been found. ~~The potential for multisite activity shown by these species is of interest in precluding and/or sidestepping the phenomena of resistance. The role of the iron generating production of ROS, is initiate, control and modulate a series of novel molecular events within cancer cells. The system is not operative on healthy cells [23]~~. Amongst the synthetized ferrocifens, the succinimido-

ferrociphenol compound p722 shows a strongest *in vitro* antiproliferative effets [24] while its *in vivo* behavior has not been evaluated so far. The exceptional antitumoral effect of this new derivative is related to the succinimide function, allowing an unprecedented stabilization of the transient quinone methide, *via* an interaction between the lone pair of one carbonyl of the heterocycle and the center of the aromatic quinone methide ring [16,24].

Considering the poor water-soluble property of ferrocifens, LNC represents a suitable drug delivery system thanks to its oily core [25]. Furthermore, encapsulation of ferrocifens enhances cellular and tumor delivery which represents an important challenge to treat cancer. ~~Thus, previous studies on LNC encapsulating ferrocifens demonstrated the efficient encapsulation and the therapeutic benefits to treat.~~ Our results confirm and improve previous findings conducted on glioblastoma [26] or melanoma [10] cells, especially concerning the characterization of nanovectors: as shown in Table 1, encapsulation efficiency, mean size, zeta potential data are consistent with formerly cited studies and these characteristics are stable over time, sustaining that these vectors are well adapted for the protocols conducted on mice models.

Several studies evaluated the cytotoxicity of ferrocifen derivatives in various tumor cell models. Thus, in a previous study, it was reported that P5 and DP1, two ferrociphenol derivatives, exerted growth inhibitory effects, mainly *via* senescence, between 0.5 and 10 µM against Hs683 and U373 human glioma cells or B16F10 mice melanoma cells [9]. Furthermore, other experiments were conducted on triple-negative MDA-MB-231 breast cancer cells for which an antiproliferative activity of ferrocifens was shown for an IC_{50} of 2.6 µM [27] and 2 µM [12]. Moreover, in a study conducted on SK-Mel28 human melanoma cells, IC_{50} was 300 nM for ferrociphenol and 1.2 mM for ansa-ferrociphenol [28] while on 9L

rat gliosarcoma cells, the IC_{50} was 0.4 and 0.6 µM for free ferrociphenol or ferrociphenol-LNC, respectively [29]. Taken together, these findings confirm a better sensitivity for p722 ferrocifen derivatives since the present study shows lower IC_{50} (168 and 187 nM for free p722 and p722-LNC, respectively) compared to previous studies. This improved sensitivity justifies the use of encapsulated p722 at lower doses, than those used in the previous studies, which will ultimately limit the toxicity.

Both *in vitro* and *in vivo* studies confirm that encapsulated p722 is able to induce apoptosis on B16F10 cells by potentiating the intrinsic pathway. Several *stimuli*, including ROS, are able to regulate apoptosis of tumor cells. Thus, as previously described, ferrocifens increase the levels of ROS in tumor cells [13] and then, could induce apoptosis. ~~Due to their reactive potential, ROS can oxidize bases, leading to DNA strand breaks, intra-strand adducts, crosslinks and mutations [30]. ROS can affect the integrity of proteins and/or lipids in membranes, decreasing the fluidity and increasing membrane permeability as well as in mitochondria [31].~~ Mitochondrial dysfunction, characterized by loss of transmembrane potential and opening of mitochondrial permeability transition pores occurs *via* many apoptotic *stimuli* [32]. Ferrocifen derivatives cause disruption of $\Delta\Psi$min breast cancer cells [13]. In melanoma, the impairment of mitochondrial membrane permits the release of cytochrome *c*, an event known to occur after externalization of phosphatidylserine [33], triggering the apoptotic intrinsic pathway with activation of caspase 9 and 3 [31]. Thus, taken together, these data suggest that the increase in caspase expression and activity, showed in this study, could be explained by an enhancement of oxidative stress induced by p722.

Numerous clinical studies [34] or pre-clinical models using several tumor cell lines of solid cancers [35,36] reveal that the combination of chemotherapy and immunotherapy enhances

survival. In metastatic melanoma, it is manifest that the combination of radiotherapy with ipilimumab (human anti-CTLA4) increases the median survival of 4 to 5 months and response rates of 25.7% *versus* 6.5% (in patients treated with ipilimumab alone) [15]. Based on these data, a part of this study aims to highlight the possible beneficial effects of a combination of anti-CTLA4 mAb and p722-LNC. We purposely chose the B16F10 model and settings of high tumor challenge ~~or delayed vaccination~~ in hopes of observing cooperative effects between blockades of multiple pathways. Yet, we are surprised that, even with double blockade, we are unable to observe any significant additive effects of these molecules in the context of metastatic melanoma: anti-CTLA4 mAb is not active in this mice model while p722-LNC has a significant therapeutic interest.

Interestingly, we confirm that p722-LNC is able to improve survival of treated mice by inducing both antitumoral effect and activation of $CD8^+$ T lymphocytes. While the pro-apoptotic properties of many ferrocifens are known [23], we identify for the first time an immune-preventative approach for p722-LNC, as it has been previously proposed ~~. A possible immunogenic cell death has been postulated with ferrocifens~~ [37]. Furthermore, these properties have been suggested with hydroxytamoxifen for which an increase of activation of Jurkat-T-cells has been shown. In this cellular model, an upregulation of cell surface markers CD28, CD69 and CD5 has been reported in hydroxytamoxifen-treated cells [38]. In the present study, a synergistic effect could explain the beneficial properties of p722. After 9 days of treatment with p722-LNC, apoptosis induced by ferrocifens could enhance the release of tumor antigens activating $CD8^+$ T lymphocytes [39] *via* antigen presenting cells. Thus, $CD8^+$ T lymphocytes could either have a direct cytotoxic activity or could constitute a pool of $CD8^+$ T memory lymphocytes explaining the significant improvement in mice survival treated with p722 [40]. Moreover, p722-LNC therapy could result in increasing

tumor infiltration of T cells and enhanced production of cytokines associated with cytotoxic T-cell function [41]. However, the precise mechanisms associated with the synergistic effects observed in the present study are not fully characterized, and mechanistic studies will be required to identify the role of different cellular subsets in the generation of effective antitumor immunity. Overall, our findings illustrate an original approach to treat metastatic melanoma through a dual property: pro-apoptotic properties and $CD8^+$ T lymphocytes activation.

These properties are identified for p722-loaded-LNC, a promising antitumor strategy. According to our data, p722 is able, on its own, to prevent the development of metastatic melanoma and to improve the survival of treated mice. However, it is important to note that the optimal schedule and dose to improve median survival in these murine models are not directly transposable in studies in humans, herein suggesting further preclinical (in other animal models) and clinical studies.

Acknowledgments

The authors wish to thank the Maine et Loire League against Cancer* for its financial support in the realization of this project. Furthermore, the authors would like to thank the French Dermatology Society for the financing of the Master program of STR. The authors thank Ms Camille Farrell Robert and Ms Isabelle Brunois-Debus for their careful editing.

*Comité départemental du Maine et Loire de la Ligue contre le Cancer

450 **References**

451 1. Ossio, R.; Roldán-Marín, R.; Martínez-Said, H.; Adams, D.J.; Robles-Espinoza, C.D.
452 Melanoma: a global perspective. *Nat Rev Cancer* **2017**, *17*, 393-394,
453 doi:10.1038/nrc.2017.43.

454 2. Garbe, C.; Peris, K.; Hauschild, A.; Saiag, P.; Middleton, M.; Bastholt, L.; Grob, J.J.;
455 Malvehy, J.; Newton-Bishop, J.; Stratigos, A.J., et al. Diagnosis and treatment of melanoma.
456 European consensus-based interdisciplinary guideline - Update 2016. *Eur J Cancer* **2016**, *63*,
457 201-217, doi:10.1016/j.ejca.2016.05.005.

458 3. Michot, J.M.; Bigenwald, C.; Champiat, S.; Collins, M.; Carbonnel, F.; Postel-Vinay, S.;
459 Berdelou, A.; Varga, A.; Bahleda, R.; Hollebecque, A., et al. Immune-related adverse events
460 with immune checkpoint blockade: a comprehensive review. *Eur J Cancer* **2016**, *54*, 139-148,
461 doi:10.1016/j.ejca.2015.11.016.

462 4. Tivol, E.A.; Borriello, F.; Schweitzer, A.N.; Lynch, W.P.; Bluestone, J.A.; Sharpe, A.H.
463 Loss of CTLA-4 leads to massive lymphoproliferation and fatal multiorgan tissue destruction,
464 revealing a critical negative regulatory role of CTLA-4. *Immunity* **1995**, *3*, 541-547,
465 doi:10.1016/1074-7613(95)90125-6.

466 5. Hughes, T.; Klairmont, M.; Sharfman, W.H.; Kaufman, H.L. Interleukin-2, Ipilimumab,
467 and Anti-PD-1: Clinical Management and the Evolving Role of Immunotherapy for the
468 Treatment of Patients With Metastatic Melanoma. *Cancer Biol Ther* **2015**, 0,
469 doi:10.1080/15384047.2015.1095401.

470 6. Lorentzen, H.F. Targeted therapy for malignant melanoma. *Curr Opin Pharmacol*
471 **2019**, *46*, 116-121, doi:10.1016/j.coph.2019.05.010.

472 7. Hodi, F.S.; O'Day, S.J.; McDermott, D.F.; Weber, R.W.; Sosman, J.A.; Haanen, J.B.;
473 Gonzalez, R.; Robert, C.; Schadendorf, D.; Hassel, J.C., et al. Improved survival with

474 ipilimumab in patients with metastatic melanoma. *N Engl J Med* **2010**, *363*, 711-723,
475 doi:10.1056/NEJMoa1003466.
476 8. Paulson, K.G.; Lahman, M.C.; Chapuis, A.G.; Brownell, I. Immunotherapy for skin
477 cancer. *Int Immunol* **2019**, *31*, 465-475, doi:10.1093/intimm/dxz012.
478 9. Bruyère, C.; Mathieu, V.; Vessières, A.; Pigeon, P.; Top, S.; Jaouen, G.; Kiss, R.
479 Ferrocifen derivatives that induce senescence in cancer cells: selected examples. *J Inorg*
480 *Biochem* **2014**, *141*, 144-151, doi:10.1016/j.jinorgbio.2014.08.015.
481 10. Resnier, P.; Galopin, N.; Sibiril, Y.; Clavreul, A.; Cayon, J.; Briganti, A.; Legras, P.;
482 Vessières, A.; Montier, T.; Jaouen, G., et al. Efficient ferrocifen anticancer drug and Bcl-2
483 gene therapy using lipid nanocapsules on human melanoma xenograft in mouse. *Pharmacol*
484 *Res* **2017**, *126*, 54-65, doi:10.1016/j.phrs.2017.01.031.
485 11. Michard, Q.; Jaouen, G.; Vessieres, A.; Bernard, B.A. Evaluation of cytotoxic
486 properties of organometallic ferrocifens on melanocytes, primary and metastatic melanoma
487 cell lines. *J Inorg Biochem* **2008**, *102*, 1980-1985, doi:10.1016/j.jinorgbio.2008.07.014.
488 12. Lainé, A.L.; Adriaenssens, E.; Vessières, A.; Jaouen, G.; Corbet, C.; Desruelles, E.;
489 Pigeon, P.; Toillon, R.A.; Passirani, C. The in vivo performance of ferrocenyl tamoxifen lipid
490 nanocapsules in xenografted triple negative breast cancer. *Biomaterials* **2013**, *34*, 6949-
491 6956, doi:10.1016/j.biomaterials.2013.05.065.
492 13. Lu, C.; Heldt, J.M.; Guille-Collignon, M.; Lemaître, F.; Jaouen, G.; Vessières, A.;
493 Amatore, C. Quantitative analyses of ROS and RNS production in breast cancer cell lines
494 incubated with ferrocifens. *ChemMedChem* **2014**, *9*, 1286-1293,
495 doi:10.1002/cmdc.201402016.

14. Allard, E.; Huynh, N.T.; Vessières, A.; Pigeon, P.; Jaouen, G.; Benoit, J.P.; Passirani, C. Dose effect activity of ferrocifen-loaded lipid nanocapsules on a 9L-glioma model. *Int J Pharm* **2009**, *379*, 317-323, doi:10.1016/j.ijpharm.2009.05.031.

15. Koller, K.M.; Mackley, H.B.; Liu, J.; Wagner, H.; Talamo, G.; Schell, T.D.; Pameijer, C.; Neves, R.I.; Anderson, B.; Kokolus, K.M., et al. Improved survival and complete response rates in patients with advanced melanoma treated with concurrent ipilimumab and radiotherapy versus ipilimumab alone. *Cancer Biol Ther* **2017**, *18*, 36-42, doi:10.1080/15384047.2016.1264543.

16. Pigeon, P.; Wang, Y.; Top, S.; Najlaoui, F.; Garcia Alvarez, M.C.; Bignon, J.; McGlinchey, M.J.; Jaouen, G. A New Series of Succinimido-ferrociphenols and Related Heterocyclic Species Induce Strong Antiproliferative Effects, Especially against Ovarian Cancer Cells Resistant to Cisplatin. *J Med Chem* **2017**, *60*, 8358-8368, doi:10.1021/acs.jmedchem.7b00743.

17. Heurtault, B.; Saulnier, P.; Pech, B.; Proust, J.E.; Benoit, J.P. A novel phase inversion-based process for the preparation of lipid nanocarriers. *Pharm Res* **2002**, *19*, 875-880.

18. Perrier, T.; Saulnier, P.; Fouchet, F.; Lautram, N.; Benoît, J.P. Post-insertion into Lipid NanoCapsules (LNCs): From experimental aspects to mechanisms. *Int J Pharm* **2010**, *396*, 204-209, doi:10.1016/j.ijpharm.2010.06.019.

19. Morille, M.; Montier, T.; Legras, P.; Carmoy, N.; Brodin, P.; Pitard, B.; Benoît, J.P.; Passirani, C. Long-circulating DNA lipid nanocapsules as new vector for passive tumor targeting. *Biomaterials* **2010**, *31*, 321-329, doi:10.1016/j.biomaterials.2009.09.044.

20. Bastiat, G.; Pritz, C.O.; Roider, C.; Fouchet, F.; Lignières, E.; Jesacher, A.; Glueckert, R.; Ritsch-Marte, M.; Schrott-Fischer, A.; Saulnier, P., et al. A new tool to ensure the fluorescent

519 dye labeling stability of nanocarriers: a real challenge for fluorescence imaging. *J Control*
520 *Release* **2013**, *170*, 334-342, doi:10.1016/j.jconrel.2013.06.014.
521 21. Zimmer, L.; Apuri, S.; Eroglu, Z.; Kottschade, L.A.; Forschner, A.; Gutzmer, R.; Schlaak,
522 M.; Heinzerling, L.; Krackhardt, A.M.; Loquai, C., et al. Ipilimumab alone or in combination
523 with nivolumab after progression on anti-PD-1 therapy in advanced melanoma. *Eur J Cancer*
524 **2017**, *75*, 47-55, doi:10.1016/j.ejca.2017.01.009.
525 22. Wolchok, J.D.; Chiarion-Sileni, V.; Gonzalez, R.; Rutkowski, P.; Grob, J.J.; Cowey, C.L.;
526 Lao, C.D.; Wagstaff, J.; Schadendorf, D.; Ferrucci, P.F., et al. Overall Survival with Combined
527 Nivolumab and Ipilimumab in Advanced Melanoma. *N Engl J Med* **2017**, *377*, 1345-1356,
528 doi:10.1056/NEJMoa1709684.
529 23. Jaouen, G.; Vessières, A.; Top, S. Ferrocifen type anti cancer drugs. *Chem Soc Rev*
530 **2015**, *44*, 8802-8817, doi:10.1039/c5cs00486a.
531 24. Wang, Y.; Pigeon, P.; Top, S.; Sanz García, J.; Troufflard, C.; Ciofini, I.; McGlinchey,
532 M.J.; Jaouen, G. Atypical Lone Pair-π Interaction with Quinone Methides in a Series of Imido-
533 Ferrociphenol Anticancer Drug Candidates. *Angew Chem Int Ed Engl* **2019**, *58*, 8421-8425,
534 doi:10.1002/anie.201902456.
535 25. Lainé, A.L.; Clavreul, A.; Rousseau, A.; Tétaud, C.; Vessieres, A.; Garcion, E.; Jaouen,
536 G.; Aubert, L.; Guilbert, M.; Benoit, J.P., et al. Inhibition of ectopic glioma tumor growth by a
537 potent ferrocenyl drug loaded into stealth lipid nanocapsules. *Nanomedicine* **2014**, *10*, 1667-
538 1677, doi:10.1016/j.nano.2014.05.002.
539 26. Karim, R.; Lepeltier, E.; Esnault, L.; Pigeon, P.; Lemaire, L.; Lépinoux-Chambaud, C.;
540 Clere, N.; Jaouen, G.; Eyer, J.; Piel, G., et al. Enhanced and preferential internalization of lipid
541 nanocapsules into human glioblastoma cells: effect of a surface-functionalizing NFL peptide.
542 *Nanoscale* **2018**, *10*, 13485-13501, doi:10.1039/c8nr02132e.

543 27. Cázares-Marinero, J.e.J.; Top, S.; Vessières, A.; Jaouen, G. Synthesis and
544 antiproliferative activity of hydroxyferrocifen hybrids against triple-negative breast cancer
545 cells. *Dalton Trans* **2014**, *43*, 817-830, doi:10.1039/c3dt52070f.
546 28. Resnier, P.; LeQuinio, P.; Lautram, N.; André, E.; Gaillard, C.; Bastiat, G.; Benoit, J.P.;
547 Passirani, C. Efficient in vitro gene therapy with PEG siRNA lipid nanocapsules for passive
548 targeting strategy in melanoma. *Biotechnol J* **2014**, *9*, 1389-1401,
549 doi:10.1002/biot.201400162.
550 29. Laine, A.L.; Huynh, N.T.; Clavreul, A.; Balzeau, J.; Béjaud, J.; Vessieres, A.; Benoit, J.P.;
551 Eyer, J.; Passirani, C. Brain tumour targeting strategies via coated ferrociphenol lipid
552 nanocapsules. *Eur J Pharm Biopharm* **2012**, *81*, 690-693, doi:10.1016/j.ejpb.2012.04.012.
553 30. Murata, M. Inflammation and cancer. *Environ Health Prev Med* **2018**, *23*, 50,
554 doi:10.1186/s12199-018-0740-1.
555 31. Obrador, E.; Liu-Smith, F.; Dellinger, R.W.; Salvador, R.; Meyskens, F.L.; Estrela, J.M.
556 Oxidative stress and antioxidants in the pathophysiology of malignant melanoma. *Biol Chem*
557 **2019**, *400*, 589-612, doi:10.1515/hsz-2018-0327.
558 32. Kroemer, G.; Galluzzi, L.; Vandenabeele, P.; Abrams, J.; Alnemri, E.S.; Baehrecke, E.H.;
559 Blagosklonny, M.V.; El-Deiry, W.S.; Golstein, P.; Green, D.R., et al. Classification of cell death:
560 recommendations of the Nomenclature Committee on Cell Death 2009. *Cell Death Differ*
561 **2009**, *16*, 3-11, doi:10.1038/cdd.2008.150.
562 33. Ford, W.E.; Ren, W.; Blackmore, P.F.; Schoenbach, K.H.; Beebe, S.J. Nanosecond
563 pulsed electric fields stimulate apoptosis without release of pro-apoptotic factors from
564 mitochondria in B16f10 melanoma. *Arch Biochem Biophys* **2010**, *497*, 82-89,
565 doi:10.1016/j.abb.2010.03.008.

34. Arriola, E.; Wheater, M.; Galea, I.; Cross, N.; Maishman, T.; Hamid, D.; Stanton, L.; Cave, J.; Geldart, T.; Mulatero, C., et al. Outcome and Biomarker Analysis from a Multicenter Phase 2 Study of Ipilimumab in Combination with Carboplatin and Etoposide as First-Line Therapy for Extensive-Stage SCLC. *J Thorac Oncol* **2016**, *11*, 1511-1521, doi:10.1016/j.jtho.2016.05.028.

35. Fritz, J.; Karakhanova, S.; Brecht, R.; Nachtigall, I.; Werner, J.; Bazhin, A.V. In vitro immunomodulatory properties of gemcitabine alone and in combination with interferon-alpha. *Immunol Lett* **2015**, *168*, 111-119, doi:10.1016/j.imlet.2015.09.017.

36. Jure-Kunkel, M.; Masters, G.; Girit, E.; Dito, G.; Lee, F.; Hunt, J.T.; Humphrey, R. Synergy between chemotherapeutic agents and CTLA-4 blockade in preclinical tumor models. *Cancer Immunol Immunother* **2013**, *62*, 1533-1545, doi:10.1007/s00262-013-1451-5.

37. Terenzi, A.; Pirker, C.; Keppler, B.K.; Berger, W. Anticancer metal drugs and immunogenic cell death. *J Inorg Biochem* **2016**, *165*, 71-79, doi:10.1016/j.jinorgbio.2016.06.021.

38. Chlichlia, K.; Moldenhauer, G.; Daniel, P.T.; Busslinger, M.; Gazzolo, L.; Schirrmacher, V.; Khazaie, K. Immediate effects of reversible HTLV-1 tax function: T-cell activation and apoptosis. *Oncogene* **1995**, *10*, 269-277.

39. Palucka, A.K.; Coussens, L.M. The Basis of Oncoimmunology. *Cell* **2016**, *164*, 1233-1247, doi:10.1016/j.cell.2016.01.049.

40. Ho, P.C.; Bihuniak, J.D.; Macintyre, A.N.; Staron, M.; Liu, X.; Amezquita, R.; Tsui, Y.C.; Cui, G.; Micevic, G.; Perales, J.C., et al. Phosphoenolpyruvate Is a Metabolic Checkpoint of Anti-tumor T Cell Responses. *Cell* **2015**, *162*, 1217-1228, doi:10.1016/j.cell.2015.08.012.

41. Wu, L.; Yun, Z.; Tagawa, T.; Rey-McIntyre, K.; de Perrot, M. CTLA-4 blockade expands infiltrating T cells and inhibits cancer cell repopulation during the intervals of chemotherapy

in murine mesothelioma. *Mol Cancer Ther* **2012**, *11*, 1809-1819, doi:10.1158/1535-7163.MCT-11-1014.

Legends

Table 1

Physico-chemical parameters and encapsulation yield of p722-LNC

Figure 1

Chemical structure of p722

Figure 2

Cytotoxicity of free p722, p722-loaded LNC on B16F10 melanoma cell line (A). Evaluation of B16F10 cell viability by MTT assay, n=3. (B) Pro-apoptotic properties of free p722, blank LNC and p722-LNC on B16F10 melanoma cell line. Evaluation of Bcl2, Bax, procaspase 9, cleaved caspase 9, procaspase 3 and cleaved caspase 3, n=3 * $p<0.05$

Figure 3

Efficacy evaluation of p722-LNC and comparison with anti-CTLA4 mAb treatment on B16F10 mice-xenografted model. (A). Evaluation of the survival of mice treated with p722-LNC compared to mice treated with blank LNC, n=6 *p=0.013 (B). Evaluation of the mice survival treated with anti-CTLA4 mAb compared to mice treated with blank LNC, n=6 (C). Evaluation of the survival of mice treated with p722-LNC compared to mice treated with anti-CTLA4 mAb, n=6 *p=0.012

Figure 4

Pro-apoptotic properties of p722-LNC. Western blot evaluation of Bcl2, Bax, procaspase 9, cleaved caspase 9, procaspase 3, cleaved caspase 3 expression, n=3. Table represents the

ratio between the expression of studied proteins and the expression of β-actin. (a) significant results compared to control mice ($p<0.05$).

Figure 5

p722-LNC activates $CD8^+$ T lymphocytes from mice tumor at day 9. (A) Evaluation of the percentage expression of $CD8^+$ T lymphocytes at day 0, day 9 and at the end of the protocol, n=6. (B) Evaluation of the percentage expression of $CD8^+$ activated T lymphocytes at D0, D9 and at the end of the protocol, n=6 * $p<0.05$.

Figure 1

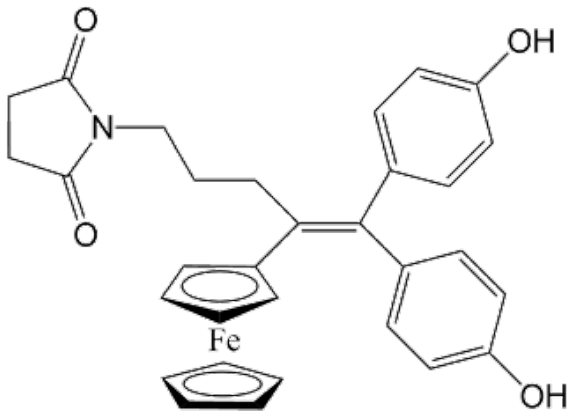

Figure 2

A

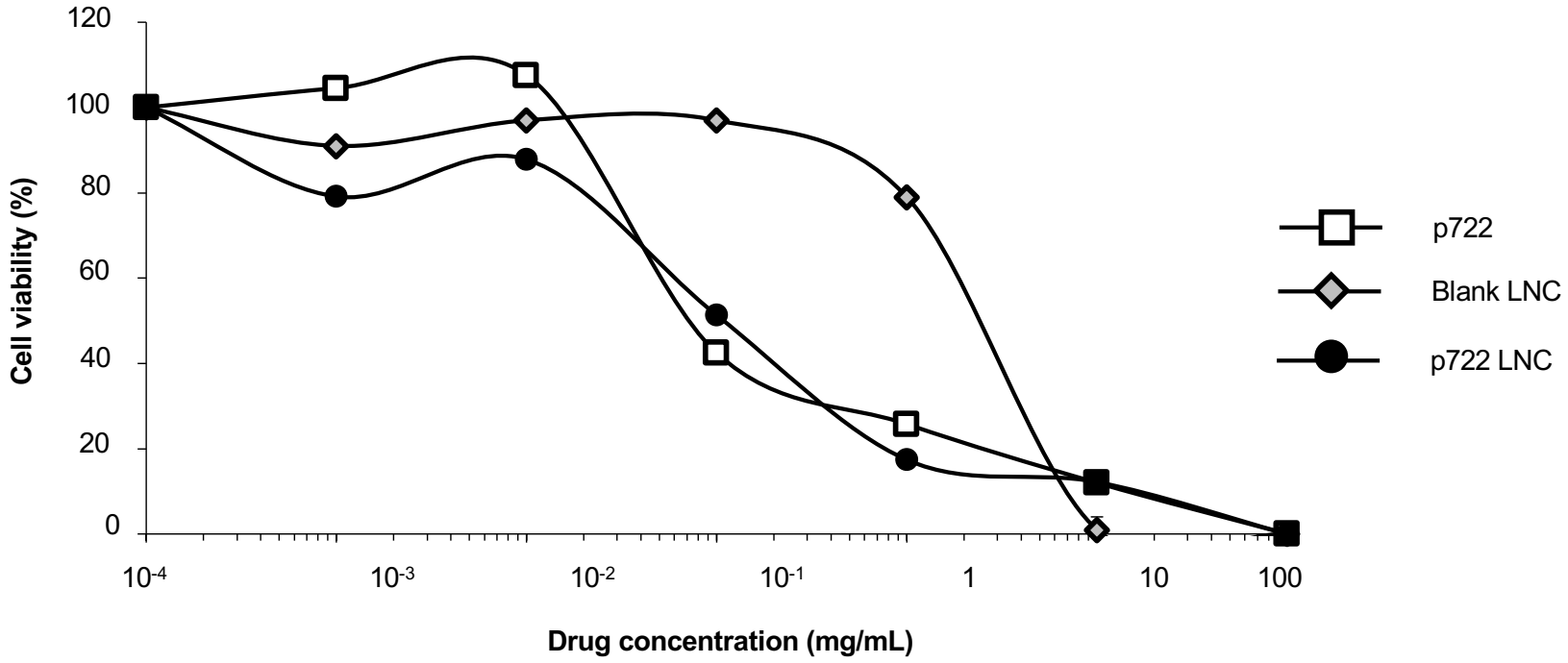

	IC50 (mg/mL)	IC50 (M)
p722	0.09	1.68×10^{-7}
Blank LNC	2.90	54.16×10^{-7}
p722 LNC	0.10	1.87×10^{-7}

Figure 2

B

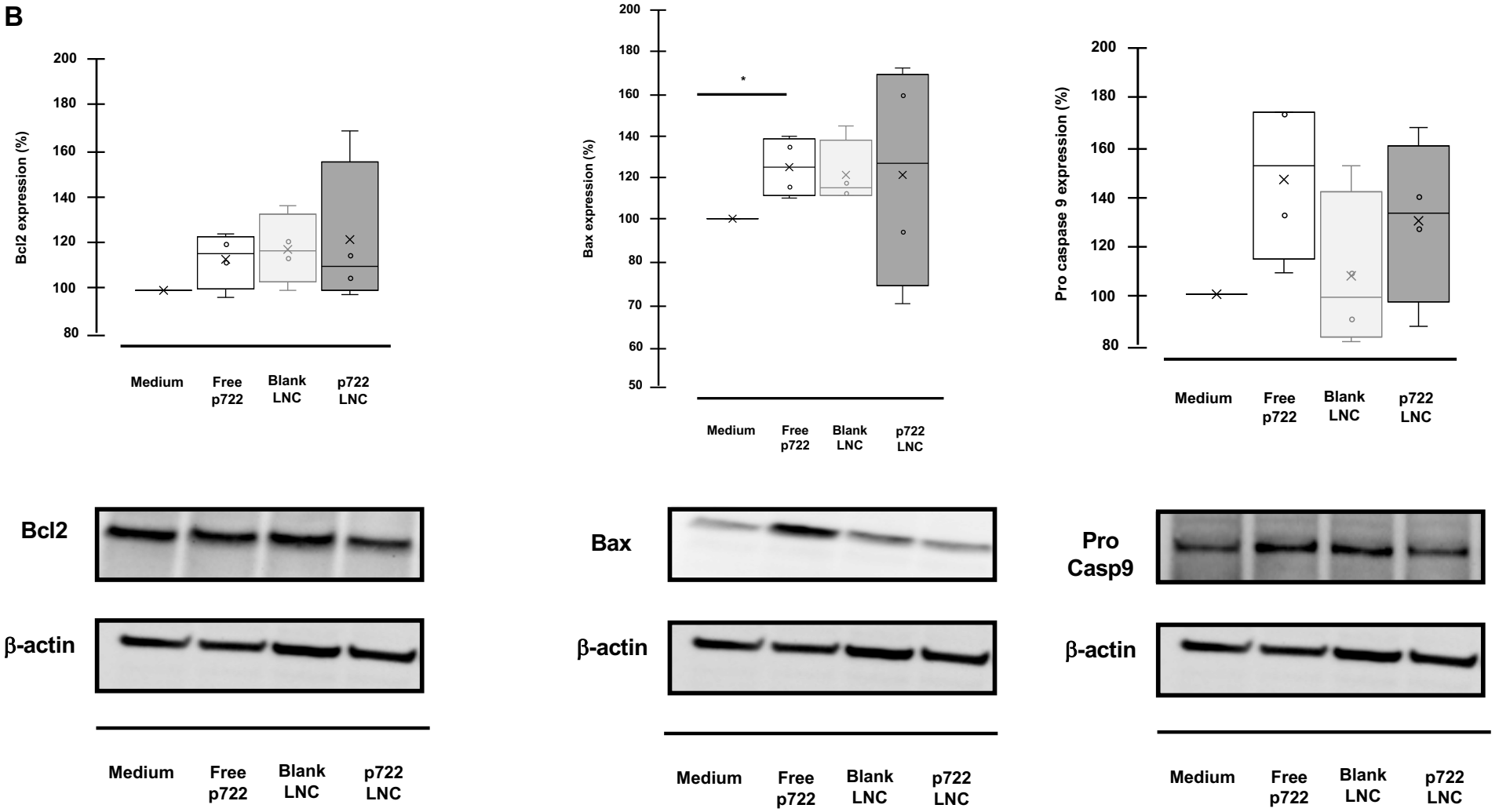
Bcl2 expression (%)
200
180
160
140
120
100
80
Medium
Free p722
Blank LNC
p722 LNC
Bax expression (%)
200
180
160
140
120
100
80
70
60
50
*
Medium
Free p722
Blank LNC
p722 LNC
Pro caspase 9 expression (%)
200
180
160
140
120
100
80
Medium
Free p722
Blank LNC
p722 LNC
Bcl2
β-actin
Medium
Free p722
Blank LNC
p722 LNC
Bax
β-actin
Medium
Free p722
Blank LNC
p722 LNC
Pro Casp9
β-actin
Medium
Free p722
Blank LNC
p722 LNC

Figure 2

B

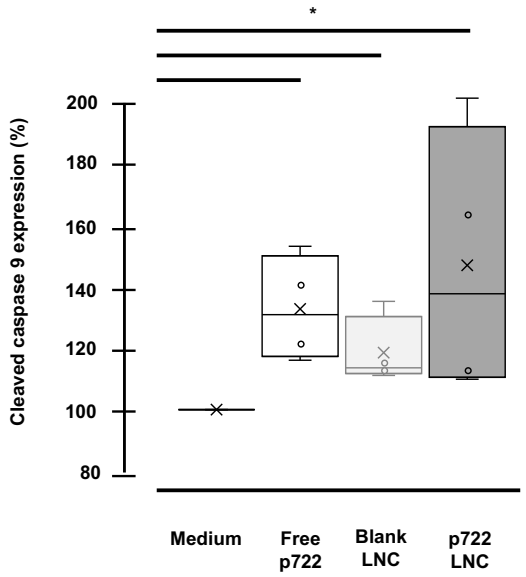
*
Cleaved caspase 9 expression (%)
200
180
160
140
120
100
80
Medium
Free p722
Blank LNC
p722 LNC

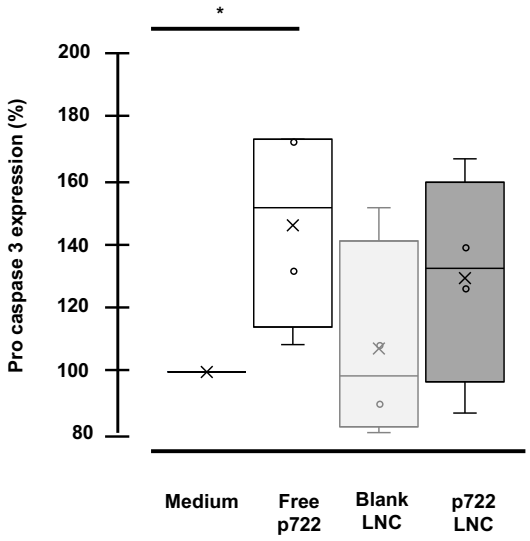
*
Pro caspase 3 expression (%)
200
180
160
140
120
100
80
Medium
Free p722
Blank LNC
p722 LNC

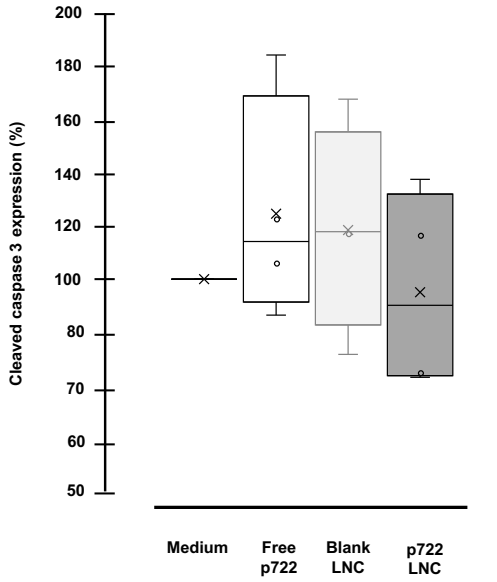
Cleaved caspase 3 expression (%)
200
180
160
140
120
100
80
70
60
50
Medium
Free p722
Blank LNC
p722 LNC

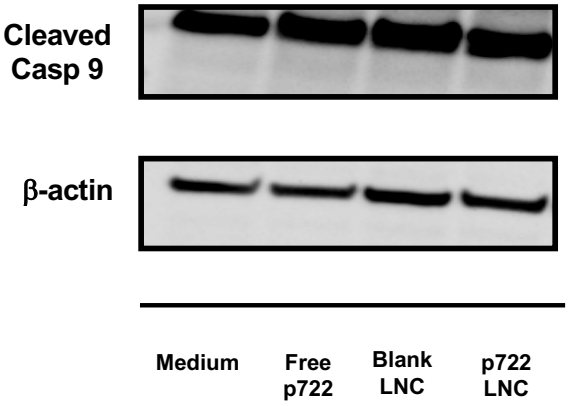
Cleaved Casp 9
β-actin
Medium
Free p722
Blank LNC
p722 LNC

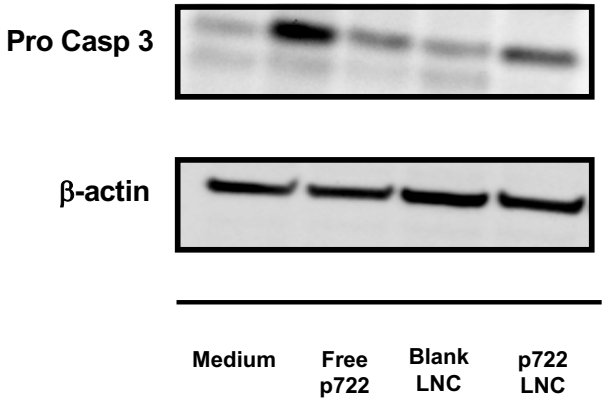
Pro Casp 3
β-actin
Medium
Free p722
Blank LNC
p722 LNC

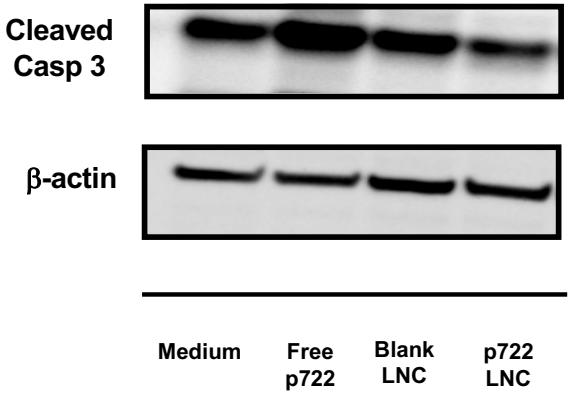
Cleaved Casp 3
β-actin
Medium
Free p722
Blank LNC
p722 LNC

Figure 3

A

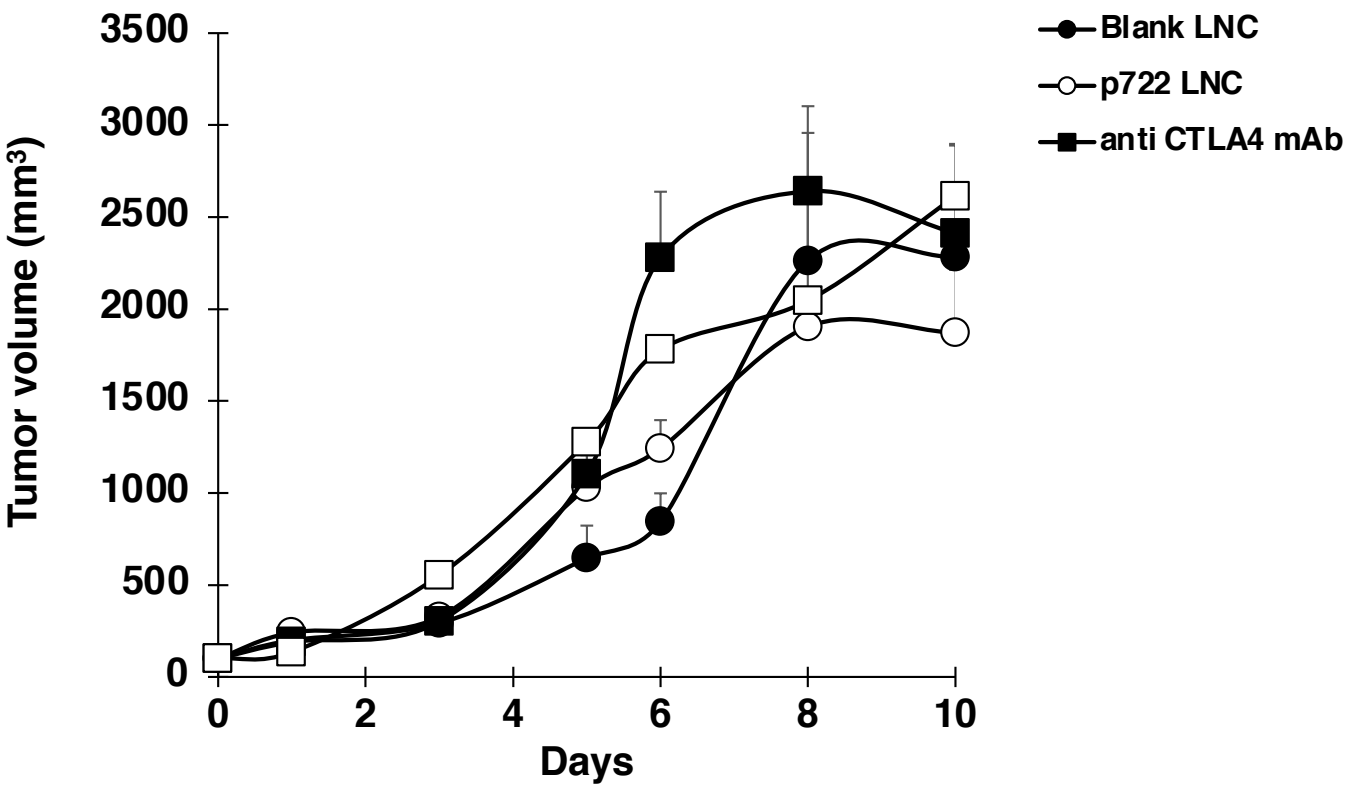
Tumor volume (mm3)
3500
3000
2500
2000
1500
1000
500
0
0
2
4
6
8
10
Days
Blank LNC
p722 LNC
anti CTLA4 mAb

Figure 3

B

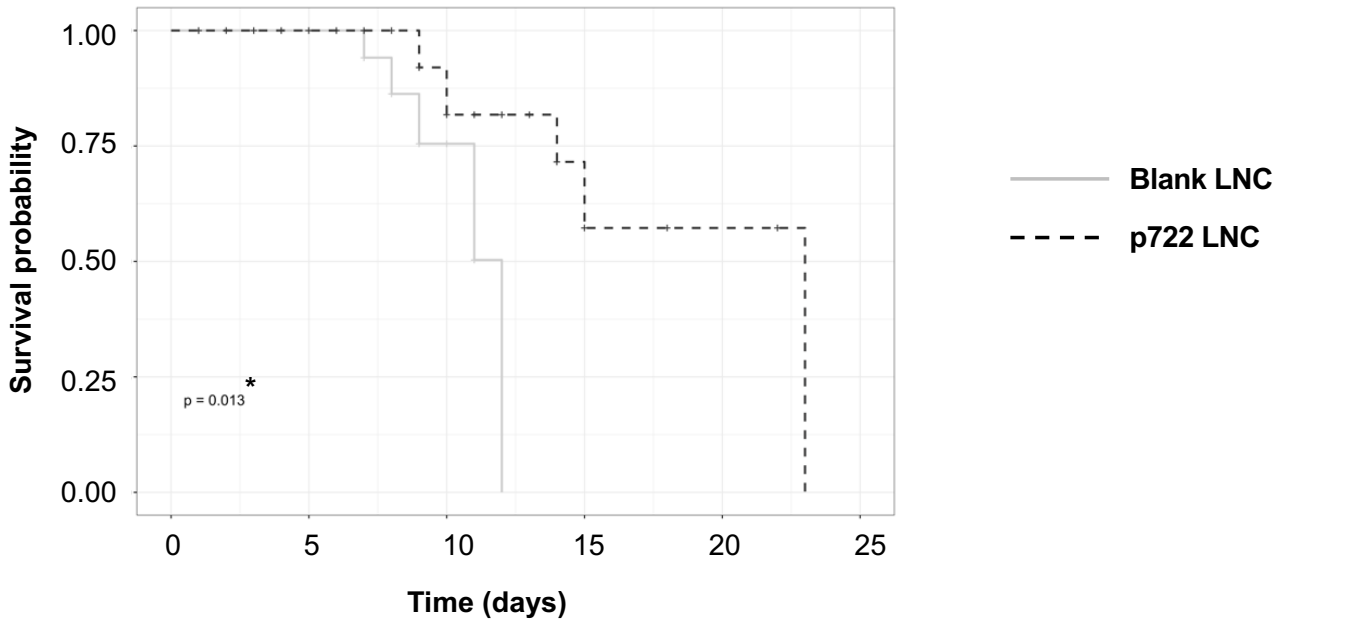
1.00
0.75
0.50
0.25
0.00
Survival probability
p = 0.013
*
0
5
10
15
20
25
Time (days)
Blank LNC
p722 LNC

C

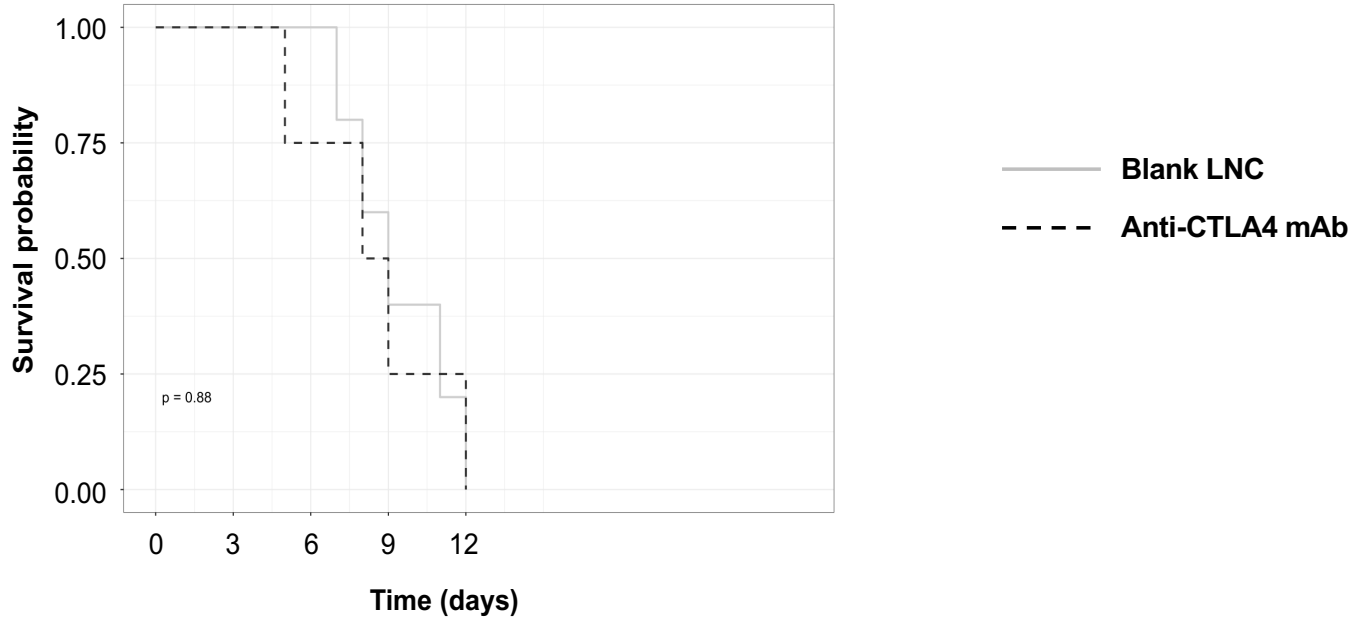
1.00
0.75
0.50
0.25
0.00
Survival probability
p = 0.88
0
3
6
9
12
Time (days)
Blank LNC
Anti-CTLA4 mAb

Figure 3

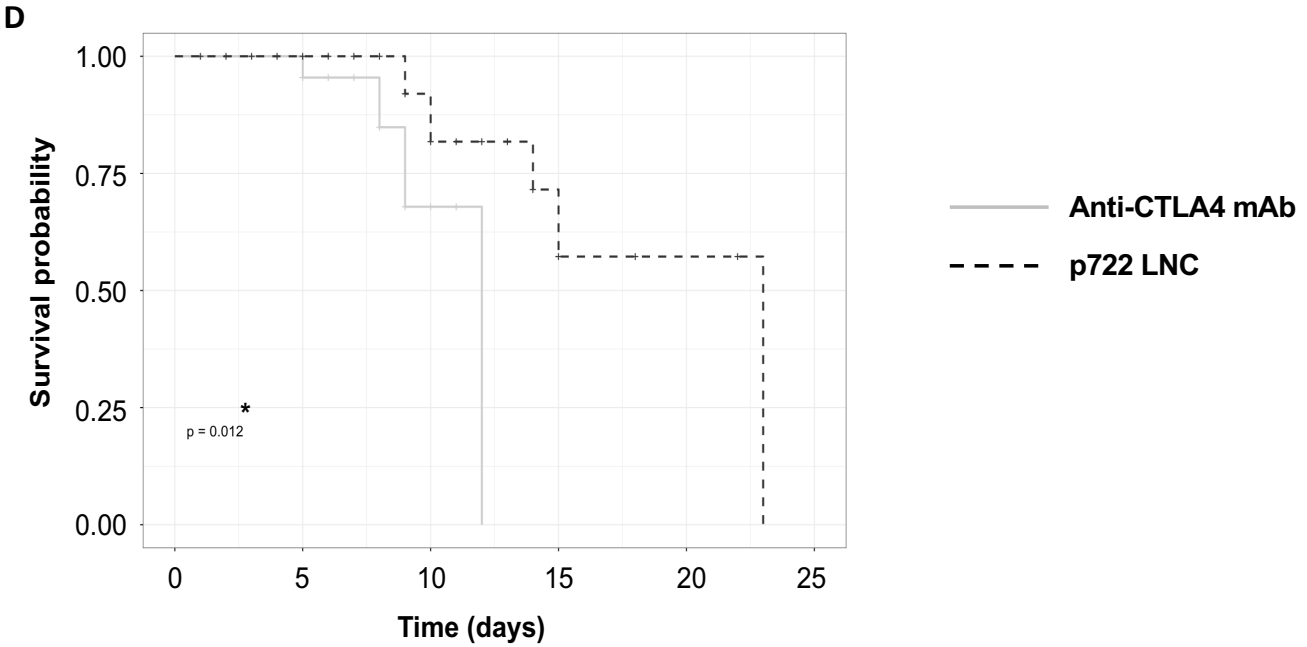
D
1.00
0.75
0.50
0.25
0.00
Survival probability
*
p = 0.012
0
5
10
15
20
25
Time (days)
Anti-CTLA4 mAb
p722 LNC

Figure 4

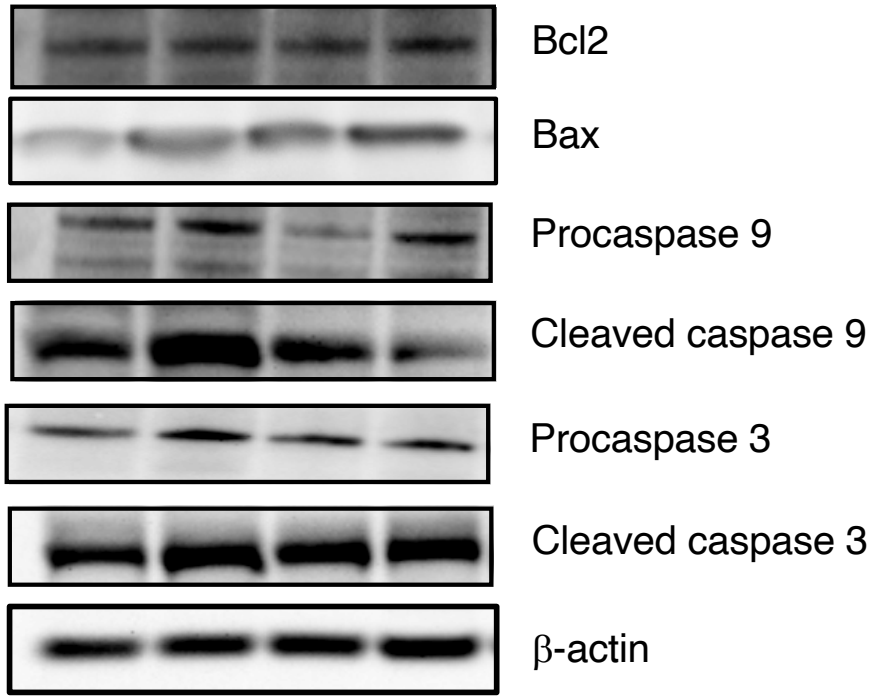

	Control	p722 LNC	mAnti-CTLA4	p722 LNC mAnti-CTLA4
BCl2	99.29 +/- 4.27	120.60 +/- 1.17	117.16 +/- 6.32	114.00 +/- 19.03
Bax	99.57 +/- 7.25	127.00 +/- 18.61	102.28 +/- 19.77	91.85 +/- 30.23
Procaspase 9	107.75 +/- 17.57	126.28 +/- 5.52[a]	115.71 +/- 23.22	103.5 +/- 25.81
Cleaved caspase 9	115.25 +/- 20.41	171.00 +/- 17.30[a]	95.00 +/- 19.00	63.66 +/- 22.81
Procaspase 3	86.61 +/- 6.54	115.00 +/- 7.22[a]	86.66 +/- 10.92	98.66 +/- 16.48
Cleaved caspase 3	98.07 +/- 7.71	236.57 +/- 66.95[a]	166.28 +/- 48.72	199.28 +/- 99.22

Figure 5

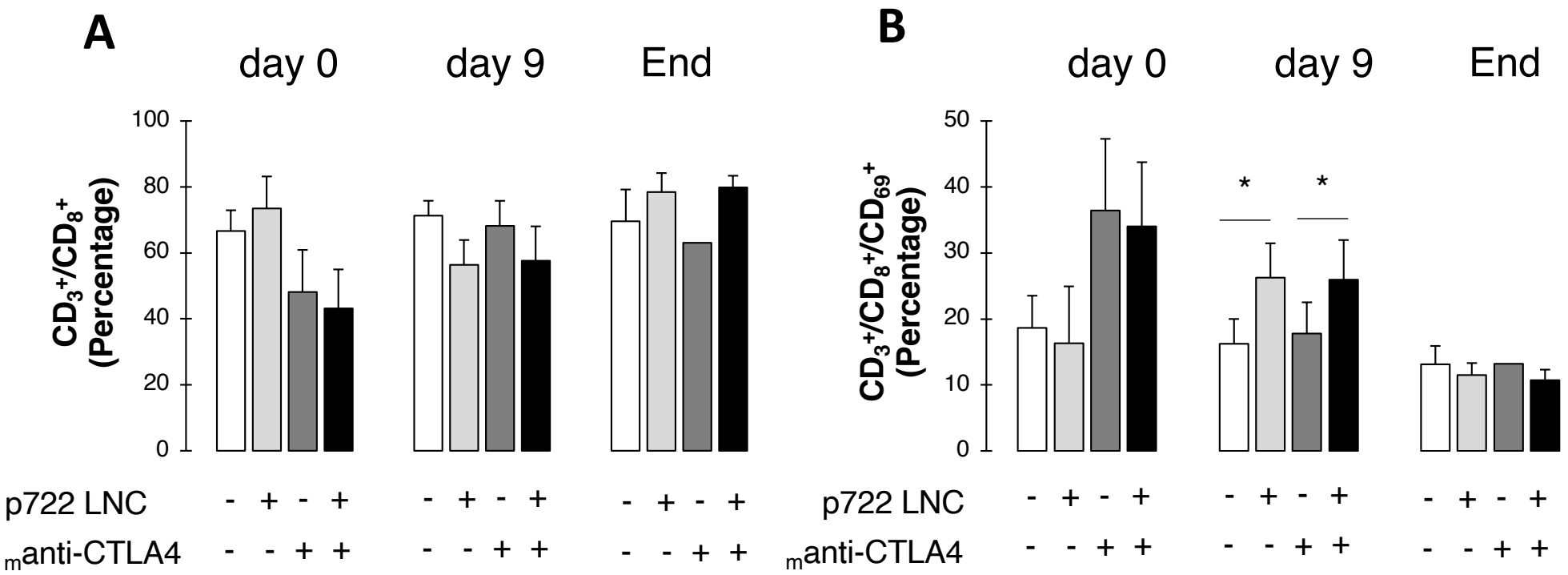
A
day 0
day 9
End
100
80
60
40
20
0
CD3+/CD8+ (Percentage)
p722 LNC - + - + - + - + - + - + - + - +
manti-CTLA4 - - + + - - + + - - + + - - + +
B
day 0
day 9
End
50
40
30
20
10
0
CD3+/CD8+/CD69+ (Percentage)
*
*
p722 LNC - + - + - + - + - + - + - + - +
manti-CTLA4 - - + + - - + + - - + + - - + +

Figure S1

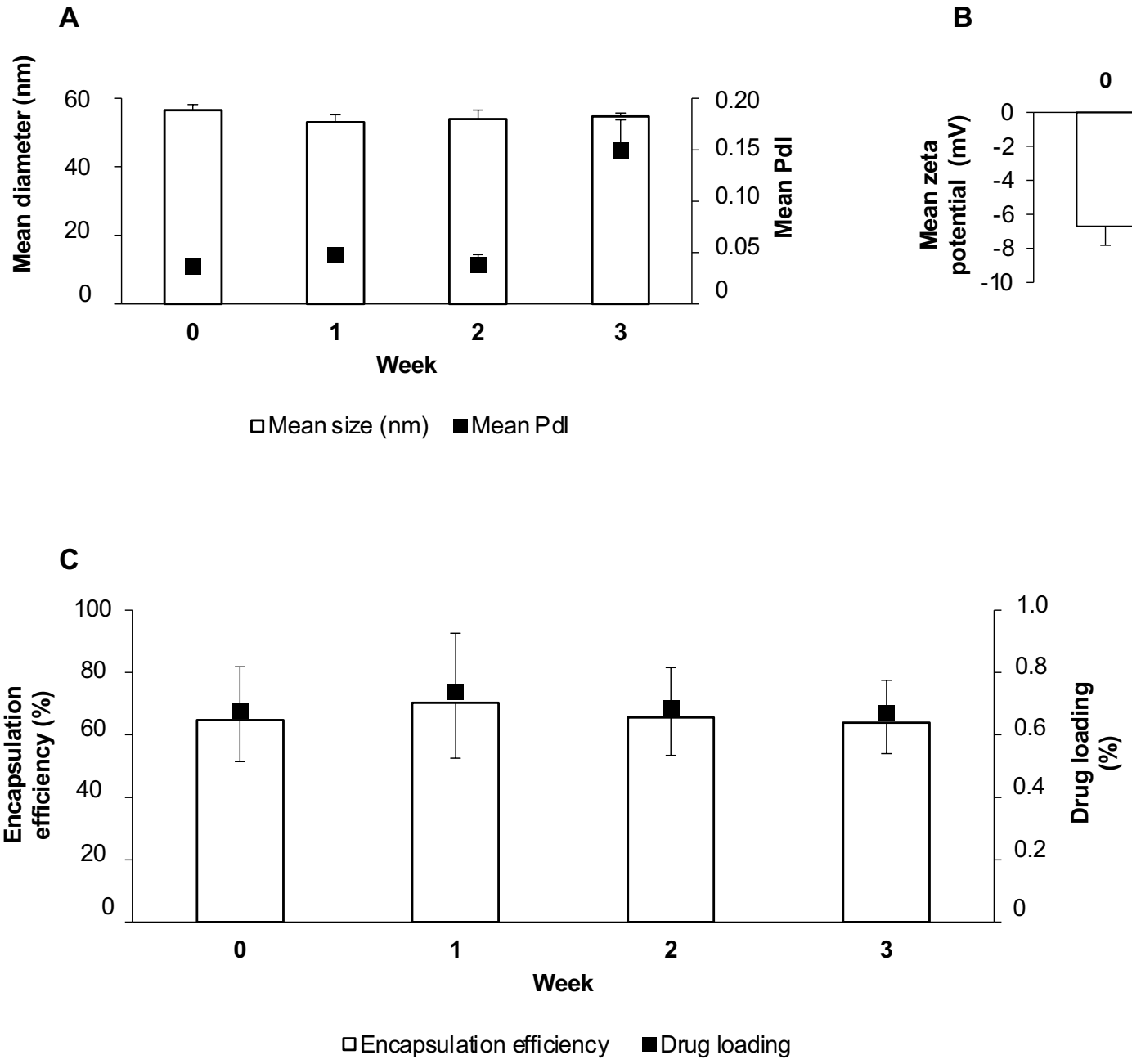
A
Mean diameter (nm)
60
40
20
0
0.20
0.15
0.10
0.05
0
Mean PdI
0
1
2
3
Week
Mean size (nm)
Mean PdI
B
Week
0
1
2
3
Mean zeta potential (mV)
0
-2
-4
-6
-8
-10
Mean zêta potential (mV)
C
Encapsulation efficiency (%)
100
80
60
40
20
0
1.0
0.8
0.6
0.4
0.2
0
Drug loading (%)
0
1
2
3
Week
Encapsulation efficiency
Drug loading

Table 1

	Mean diameter (nm)	Mean PdI	Mean zeta potential (mV)	EE (%)	Drug loading (%)
Blank pegylated-LNC	72.4 +/- 0.8	0.12 +/- 0.01	-29.0 +/- 1.2	/	/
p722 pegylated-LNC [2.25 mM]	70.0 +/- 1.0	0.15 +/- 0.01	-13.5 +/- 0.5	64.8 +/- 13.4	0.7 +/- 0.1

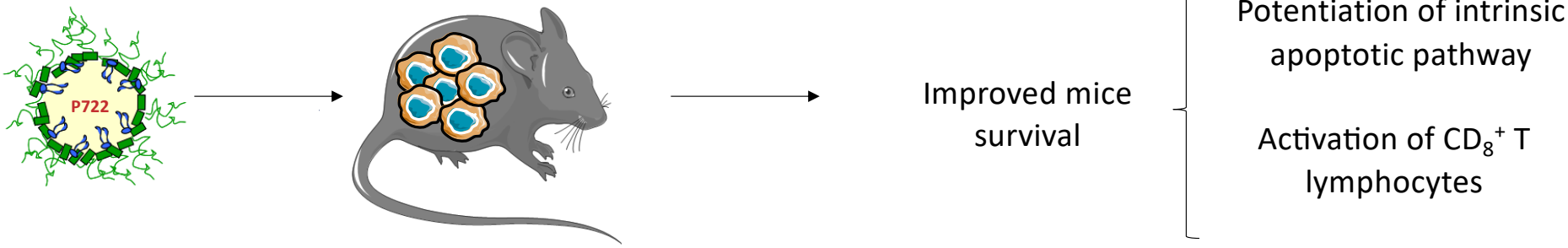
P722
Improved mice survival
Potentiation of intrinsic apoptotic pathway
Activation of CD_8^+ T lymphocytes